# Biallelic variants in ERLIN1: a series of 13 individuals with spastic paraparesis

Guillaume Cogan, Maha S Zaki, Mahmoud Issa, Boris Keren, Marine Guillaud-Bataille, Florence Renaldo, Arnaud Isapof, Pauline Lallemant, Giovanni Stevanin, Lena Guillot-Noel, et al.

# Biallelic variants in *ERLIN1*: a series of 13 individuals with spastic paraparesis

Guillaume Cogan[1], Maha S. Zaki[2], Mahmoud Issa[2], Boris Keren[1], Marine Guillaud-Bataille[1], Florence Renaldo[3], Arnaud Isapof[3], Pauline Lallemant[4,7], Giovanni Stevanin[7,8], Lena Guillot-Noel[7], Thomas Courtin[1], Julien Buratti[1], Cécile Freihuber[3], Joseph G. Gleeson[5,6], Robyn Howarth[5,6], Alexandra Durr[7], Jean-Madeleine de Sainte Agathe[1], Cyril Mignot[1,7]

[1]APHP Sorbonne Université, Département de Génétique, Groupe Hospitalier Pitié-Salpêtrière-Hôpital Trousseau, Centre de Référence Déficiences Intellectuelles de Causes Rares, ERN-ITHACA, Paris, France.
[2]Clinical Genetics Department, Human Genetics and Genome Research Institute, National Research Centre, Cairo, Egypt.
[3]APHP Sorbonne Université, Service de Neuropédiatrie, Centre de Référence Neurogénétique, Hôpital Armand Trousseau, Paris, France.
[4]APHP Sorbonne Université, Service de Médecine Physique et de Réadaptation pédiatrique, Hôpital Armand Trousseau, Paris, France.
[5]Department of Neurosciences, University of California, San Diego, La Jolla, CA 92093, USA
[6]Rady Children's Institute for Genomic Medicine, San Diego, CA 92130, USA
[7]Sorbonne Université, Institut du Cerveau - Paris Brain Institute ICM, Inserm, CNRS, APHP, Hôpital de la Pitié Salpêtrière, Paris, France
[8] Bordeaux University, INCIA, UMR5287, CNRS, EPHE, 33000 Bordeaux, France

**Corresponding author:**
Dr. Cyril Mignot, Département de Génétique, Groupe Hospitalier Pitié-Salpêtrière, 47-83 Boulevard de l'hôpital, 75013 Paris, France
Email address: cyril.mignot@aphp.fr

**Acknowledgments:**
We thank the participants for taking part in this study. This work was partially funded by the Egyptian National Research Centre, project number: 13060169, with local Medical Research Ethical committee approval number 2-3-6 for the year 2023. We

also thank Sarah Boster for the help in improving the English quality of the manuscript.

**ABSTRACT**

Biallelic variants in the *ERLIN1* gene were recently reported as the cause of two motor neuron degeneration diseases, SPG62 and a recessive form of amyotrophic lateral sclerosis. However, only 12 individuals from five pedigrees have been identified so far. Thus, the description of the disease remains limited. Following the discovery of a homozygous pathogenic variant in a girl with SPG62, presenting with intellectual disability, and epilepsy, we gathered the largest series of SPG62 cases reported so far (13 individuals) to better understand the phenotype associated with *ERLIN1*. We collected molecular and clinical data for 13 individuals from six families with *ERLIN1* biallelic variants. We performed RNA-seq analyses to characterize intronic variants and used Alphafold and a transcripts database to characterize the molecular consequences of the variants. We identified three new variants suspected to alter the bell-shaped ring formed by the ERLIN1/ERLIN2 complex. Affected individuals had childhood-onset paraparesis with slow progression. Six individuals presented with gait ataxia and three had superficial sensory loss. Aside from our proband, none had intellectual disability or epilepsy. Biallelic pathogenic *ERLIN1* variants induce a rare, predominantly pure, spastic paraparesis, with possible cerebellar and peripheral nerve involvement.

**Keywords:**

ERLIN1, spastic paraplegia, intronic variants, RNA-Seq, 3D protein structure

## INTRODUCTION

The *ERLIN1* (Endoplasmic Reticulum lipid raft associated protein 1) gene encodes a transmembrane endoplasmic reticulum (ER) glycoprotein composed of 348-amino acids widely expressed in human tissues (Fagerberg et al. 2014). The ERLIN1 protein shares 83% of its sequence identity with ERLIN2. Their assembly is mediated at two levels: the primary interactions between “assembly domains” (residues 301-311 in ERLIN1 and 299-309 in ERLIN2) and coiled-coil regions (residues 179-276 in ERLIN1 and 177-274 in ERLIN2) which form lower-order hetero-oligomers; these then associate at the ER membrane to form the higher-order ring-shaped heteromultimeric ERLIN1/2 complex, composed of ~ 40 subunits in a ~ 1:1 ratio (Manganelli et al. 2021; Pednekar et al. 2011) (Figure 1).

Both proteins belong to the prohibitin family by virtue of a conserved prohibitin-homology domain (PHB) of ~160 amino acids (Browman et al. 2006). The ERLIN1/2 complex participates in the formation of specialized raft-like microdomains regulating intracellular trafficking and sorting (Helms et Zurzolo 2004), cholesterol homeostasis (Ouweneel, Thomas, et Sorci-Thomas 2020), cell survival and death (Young, Kester, et Wang 2013). More specifically, the ERLIN1/2 complex is involved in the degradation of misfolded proteins located in the ER lumen by the proteasome through the ER-associated protein degradation (ERAD) pathway (Pearce et al. 2007; Stevenson, Huang, et Olzmann 2016). It associates with the RNF170 ubiquitin ligase E3 to degrade the activated inositol 1,4,5 triphosphate receptor (IP3R) (Pearce et al. 2007; 2009). The finding that biallelic pathogenic variants in *ERLIN2* (Alazami et al. 2011), *ERLIN1* (Novarino et al. 2014) and *RNF170* (Wagner et al. 2019) are responsible for recessive hereditary spastic paraparesis (HSP), coined as SPG18B (OMIM 611225), SPG62 (OMIM 615681) and SPG85 (OMIM 619686), respectively, demonstrates that motor neurons are sensitive to this degradation process. The accumulation of the Ca+ channel IP3R could be the prominent pathophysiological mechanism (Gao et Wojcikiewicz 2020).

Biallelic *ERLIN1* pathogenic variants were first reported in seven individuals from three families with SPG62 (Novarino et al. 2014). Four years later, *ERLIN1* mutations were identified in four individuals from a single family with amyotrophic lateral sclerosis (ALS) (Tunca et al. 2018). Finally, a twelfth person with SPG62 has recently been

identified (Zhu et al. 2022). Epilepsy and intellectual disability (ID) were not reported for any of these individuals. As is the case for some other HSPs (Iskender et al. 2015; Parodi et al. 2017), Tunca et al. suggested that *ERLIN1*-related motor neuron degeneration could involve upper motor neurons first and later evolve to the loss or dysfunction of lower motor neurons, with symptoms such as muscle atrophy and weakness. The latter could mislead clinicians to diagnose ALS (Tunca et al. 2018). All reported variants were homozygous, either nonsense (p.Arg255*), missense (p.Gly50Val), splice site (c.504+1G>A) or delins (p.YQA288_290delinsS) in HSP, while a missense variant (p.Val94Ala) was found in the one reported ALS family. A partial or complete loss-of-function is the most likely consequence of these changes, disturbing the formation of the ERLIN1/2 complex.

The current study focuses on 13 new individuals with SPG62 due to homozygous mutations in *ERLIN1.* We have identified new pathogenic variants and explored whether the *ERLIN1*-phenotype spectrum is broader than previously suspected.

## MATERIALS AND METHODS

### 1. Participants

We first identified (ES) the homozygous c.430+3_430+6del *ERLIN1* intronic variant in Individual 1 presenting with HSP, epilepsy and ID through exome sequencing (ES). As few individuals with this variant had been previously identified and had neither epilepsy nor ID, we collected new patients to further characterize the *ERLIN1* phenotype. We collected retrospective clinical and molecular data from patients with biallelic pathogenic *ERLIN1* variants included in the SPATAX registry who were located at the Paris Brain Institute (ethical institutional review board authorization RBM-029) and through collaborative calls (GeneMatcher (Sobreira et al. 2015) and the European Rare Diseases Network ITHACA). This approach led to the identification of 12 additional affected cases. Participating neurologists referred cases and were asked to fill out a questionnaire to collect clinical and molecular data.

### 2. DNA sequencing and analyses

**Families I, II and III (individuals 1-5).** Exome sequencing was performed on DNA isolated from the blood of the probands and their parents. Genomic DNA was extracted from peripheral blood lymphocytes using a Qiasymphony DNA Midi Kit (Qiagen). A SeqCap EZ MedExome Library kit (NimbleGen, Roche Sequencing) was used for

genomic capture. A NextSeq 500 Sequencer was used for massive parallel sequencing. Raw data was analyzed with in-house annotation and analysis pipelines. For data analysis, raw reads were mapped to the human genome reference-build hg19 using the Burrows Wheeler Aligner (BWA MEM v0.717) alignment algorithm. The resulting binary alignment/map (BAM) files were further processed by Genome Analysis Tool Kit HaplotypeCaller (GATK HC v3.8). The VCF files were then annotated on Snpeff version 4.3T. Finally, the variants were identified according to in house protocol: (i) only coding nonsynonymous and splicing variants were considered, and (ii) variant filtration was conducted according to the transmission mode (de novo, autosomal recessive and X-linked), frequency of the variant in the gnomAD database (S et al. 2024).

**Families IV and V (Individuals 6-11)**. Genome sequencing (GS) was performed from blood samples as described (Kingsmore et al. 2020) with 2 × 101 nt and a depth of more than 30 fold (Illumina). Read alignment to *GRCh37* and variant diplotype identification was carried out with DRAGEN (Illumina) and included copy number and structural variant identification. Semiautomated interpretation was performed using MOON (InVitae), GEM, and Enterprise (Fabric Genomics) as described (Kircher et al. 2014; Wiel et al. 2019). Inputs were variant call files, manually curated lists of observed human phenotype ontology terms, and metadata. Reportable diplotypes were identified by filtering and ranking disease phenotype match, variant pathogenicity, and rarity using decision trees, bayesian models, neural networks, and natural language processing. The final classification was performed according to the American College of Medical Genetics and Genomics guidelines by molecular laboratory directors (Kircher et al. 2014), as was the case for exome sequencing of individuals 1, 2, 3, 4, 5.

**Family VI (individuals 12 and 13).** Genomic DNA was extracted from peripheral blood samples using standard procedures. ES with DNA samples was performed as previously described (von Elsner et al. 2021). To summarize, coding DNA fragments were enriched with the SureSelect Human All Exon V6 kit (Agilent), and captured libraries were then loaded and sequenced on the HiSeq platform (Illumina). Reads were aligned to the human reference genome (UCSC GRCh37/hg19) using the Burrows-Wheeler Aligner (BWA mem, v0.7.17-r1188). Genetic variants were detected with the Genome Analysis Toolkit (GATK, v3.8) and annotated using AnnoVar (v2018-04–16). Only private (absent in public database) and rare (with minor allele frequency <0.1% and not present in the homozygous state in public databases or the parents)

exonic and intronic variants at exon-intron boundaries ranging from −10 to +10 were retained. The remaining variants were then prioritized by pathogenicity assessment using multiple *in silico* tools (CADD, REVEL, M-CAP, Human Splicing Finder 3.1, NetGene2-Server, and Berkeley Drosophila Genome Project-Database).
We used RefSeq NM_006459.4 as the relevant reference sequence.

3. Splicing analysis with RNA-seq and RT-PCR

**Individual 1.** RNA from Individual 1 and controls was extracted either from blood or fibroblast, using PAXgene (PreAnalytiX) blood RNA tubes with PAXgene blood RNA kit or the RNeasy plus mini kit (Qiagen, Düsseldorf, Germany), respectively.
RNA sequencing was performed using the mRNA stranded kit (Illumina, San Diego, CA, USA). Strand-specific sequencing libraries were prepared using Illumina Stranded mRNA Prep. Paired-end 75-bp sequencing was performed on the NextSeq 500 Illumina platform, demultiplexing and raw sequences were obtained using Illumina's bcl2fastq. Reads were mapped to the GRCh38 human reference genome using STAR software and analyzed using Integrative Genomics Viewer (IGV). Global quality was assessed using FastQC, RNA-SeQC, Picard Tools and MultiQC.
**Individual 3 and 4.** RNA was extracted from lymphoblast cell pellets, treated with and without emetine, using the QIAGEN "RNeasy Plus Minit Kit". The RT-PCR was performed using the BIO-RAD kit "iScript Reverse Transcription Supermix for RT-qPCR". The region of interest was amplified for individuals II-3 and II-4 using PCR with primers designed with Primer3 (Figure S1). The forward primer was located in exon 5 and the reverse primer in exon 6. We obtained the full sequence for the region using Ensembl (https://www.ensembl.org). The specificity of the primers was verified using UCSC blat function (https://genome.ucsc.edu/). RNA was migrated on the Caliper LabChip GX.
**Individual 7 and carrier relative**. Total RNA was extracted (Monarch Total RNA Miniprep Kit, New England Biolabs) from fibroblasts from Individual 5 and a carrier family member. Samples were assessed for purity and RNA concentration using the Epoch™ Microplate Spectrophotometer (BioTek). RNA sequencing was carried out using polyA-enriched RNA sequencing (TruSeq Stranded mRNA Kit, Illumina). Paired-end sequencing (2 × 100 bp) was performed with an Illumina NovaSeq 6000 instrument at a sequencing depth of 60–100 million paired reads per sample and a minimum output of 12 Gb per sample. Output bcl files were converted to fastq files and

demultiplexed using bcl2fastq (v2.20, Illumina). Adapter trimming was performed with Skewer (v0.2.2). Sequence reads were aligned to the human reference genome assembly (GRCh38.98) using STAR (v2.7.3a) in two-pass mode. We used LeafCutter (v0.2.9) for the detection and quantification of novel and known alternative splicing events. For differential intron excision analysis, the required minimum number of samples supporting an intron and the minimum number of samples per group was reduced to 1. Differentially spliced clusters with a false discovery rate (FDR) of 0.1 were visualized as Sashimi plots.

4. Protein structure modeling

Erlin1/2 tetramer was generated with alphafold2, using alphafold2_multimer_v3 from ColabFold, based on the full ERLIN1 and ERLIN2 human sequences, respectively uniprot: O75477 and O94905. The figures were made with Mol*.

**RESULTS**

1. *ERLIN1* variants

In total, we identified three different homozygous intronic *ERLIN1* variants in six families comprising 13 individuals with HSP (Table 1 and Figure 2A). All affected individuals carried the homozygous variant found in their respective families. All variants were unreported as homozygous in gnomAD (v.4), absent in ClinVar and HGMD databases, and met the ACMG classification criteria as “likely pathogenic” or “pathogenic”.

They were all predicted to alter splicing by Spip and SpliceAI (Jm et al. 2023; « Predicting Splicing from Primary Sequence with Deep Learning - PubMed », s. d.). RNA-seq and RT-PCR analyses confirmed that the recurrent c.430+3_430+6del variant, found in six individuals from four families, led to a skipping of exon 5 (r.430+3_430+6del), and that skipping of exon 7 resulted from the c.505-14C>G change (r.505-14c>g) (Figure 2B, 2C and Figure S1, Table S1). RNA-seq was not performed for c.430+1G>T, but it alters the canonical splice site, thus it likely leads to a loss of a donor splice site and the skipping of exon 5, as predicted by SpliceAI (score 1) and by Spip (98% risk of alteration) (Figure S2).

2. Pyramidal syndrome and disease progression

Of the 13 affected individuals, nine females and four males were seen at a mean age of 19.3 years (range 2-40, median 18) at last examination. All originated from North Africa and/or the Middle East. All of the pregnancies were uneventful with the exception of one where hypertension was present during the pregnancy. Birth measurements, when available, were all within the normal range.

When reported, the first signs of motor involvement occurred before the age of 5, (mean 1.8 years, range 9 months – 4 years). In 5/9 individuals, walking delay and abnormal gait were the first manifestations of the disease and were observed prior to age 2. Stiffness of the lower limbs and spastic gait became obvious at 7 years of age at the latest. The disease worsened over time, at a different rate from one individual to another. Disease course was the slowest in Individual 2 who had stiff legs starting at age 1, and only mild difficulties with running and walking at 7 years old. By age 22, he was unable to run and had limited walking ability. In contrast, Individual 1, with the most severe progression, had spastic paraparesis in their second year of life and used a wheelchair at age 9 for long-distances. Generally, individuals needed walking assistance, either walking with crutches or a wheelchair, before the end of their second decade. At the last examination, all individuals had lower limb spasticity, brisk tendon reflexes, equinovarus deformity, bilateral Babinski sign, and ankle clonus but no involvement of the upper limbs.

3. Associated signs

Signs of cerebellar involvement, primarily gait ataxia combined with progressive pyramidal signs, were noted on examination in six individuals. One of these people also exhibited slow saccades and horizontal gaze nystagmus. These individuals carried either the c.505-14C>G or the c.430+3_430+6del variant. Superficial sensory loss (3/13) was reported for three individuals from the same family with the c.430+3_430+6del variant but nerve conduction velocity could not be recorded.

Urinary disturbances, swallowing difficulties, hyperlaxity, and scoliosis were reported for one person each. Height and occipitofrontal circumference were within the normal range for most individuals.

Cerebral MRI was normal for three individuals and showed a thin corpus callosum (TCC) in five individuals from three distinct families (II – III – V) with two genotypes (c.430+3_430+6delAAGT and c.505-14C>G) (Figure S3). One person had vermian and hemispheric cerebellar atrophy associated with bilateral pontine hypersignal at

age 22 (images not available). Two patients under ten years old underwent electromyogram/nerve conduction velocity recording with normal results.

The phenotype in Individual 1 carrying the recurrent c.430+3_430+6del variant showed a combination of the most severe form of spastic paraparesis of the series and mild/moderate ID (WISC-V full scale intellectual quotient 60). She had significant behavioral problems with a diagnosis of attention deficit and hyperactivity disorder as well as levetiracetam-responsive absence seizures starting at age 6.5 despite a normal brain MRI (Figure S3). Individuals 5 and 6 presented with learning difficulties, with psychometric tests showing heterogeneous abilities in Individual 5 (WISC-V, verbal comprehension index 65, fluid reasoning index 85, visual spatial index 86, working memory index 79, and processing speed index 95) at 10 years old.

## DISCUSSION

Up until now, biallelic *ERLIN1* variants had been reported in 12 individuals with two overlapping phenotypes, SPG62 (n=8) (Zhu et al. 2022) and ALS (n=4 in a single family) (Tunca et al. 2018). Our study contributes to the characterization of *ERLIN1*-associated phenotypes by describing three novel intronic variants in 13 newly discovered individuals.

1/ Depicting the genotype landscape of *ERLIN1*

Prohibitin proteins share common characteristics. They tend to form oligomers and have an alpha-helical stretch (residues 179-276 in *ERLIN1*) which can lead to coiled-coil motifs (Pearce et al. 2009). Reported genetic variants to date were either stopgain, splice site, delins or missense. In contrast, the three variants reported here were intronic, either located in intron 5 (2/3) or intron 6 (1/3), according to the canonical transcript NM_006459.4.

RNA-seq performed in c.430+3_430+6del and c.505-14C>G showed skipping of exon 5 (c.305_430) and exon 7 (c.504_562), respectively (Figure 2B). c.430+1G>T is predicted by spliceAI to induce exon 5 skipping by loss of the canonical donor site (Figure S2). Exon 7 deletion results in a frameshift (p.Ala169Glyfs*3) (Figure 2C) and Zhu et al. have previously shown that the loss of exon 7 (confirmed by RNAseq and minigene) contributes to SPG62 (Zhu et al. 2022). Interestingly, exon 5 deletion is inframe (p.Val102_Phe143del) which opens new avenues regarding the potential

molecular mechanisms involved in SPG62. To date, no deletion fully encompassing exon 5 had been reported in both the Database of Genomic Variants and gnomAD SVs (v.4). Deletions reported in the Decipher database encompass all coding sequences of *ERLIN1* and neighbor genes.

Currently, there is no cryo-EM structure for the ERLIN1/2 complex. Thus, we relied on a recently identified bacterial stomatin/prohibitin/flotillin/HflK/C (SPFH) domain containing bacterial proteins sharing homology with Erlin1 and Erlin2 to further model the consequences of variants in the ERLIN1 protein, as had previously been done in the literature (Gao et Wojcikiewicz 2020; Ma et al. 2022; Daumke et Lewin 2022). Based on alpha-fold 3D Erlin1 and Erlin2 predicted structure, ERLIN1/2 complex likely forms a similar structure as the “bell-shaped” cage of the FtsH complex of E.Coli (Figure 1) (Ma et al. 2022). This complex is anchored to a double layer membrane. In-frame exon 5 deletion, along with exon 7 frameshift deletion, are located in the PHB domain (Figure 2C). They likely impair the lower-order hetero-oligomerization of ERLIN1 and ERLIN2 and subsequently disrupt the “bell-shaped” cage structure formed by the higher-order ERLIN1/2 complex, finally impairing the capacity of ERAD to degrade targeted misfolded proteins and activated IP3Rs.

2/ The phenotype landscape of SPG62

Early-onset ALS, starting from the second decade of life, has previously been described in one family with the homozygous p.Val94Ala *ERLIN1* variant (Tunca et al. 2018). Lower motor neuron degeneration was not a feature in our series. Of note, the number of patients who have had peripheral nerve studies remains limited, and when available, examinations were performed at a very young age. These data suggest that ALS is a rare manifestation of biallelic *ERLIN1* variants, or a late-onset feature of the disease course in SPG62, or both.

Our cohort confirms the early onset of SPG62, with a mean age of 1.8 years (9 months – 4 years old) when manifestations were first observed, and younger than previously described in the literature (mean age at onset 4.8 years, range 17 months – 13 years old). SPG62 disease progression appears to be relatively slow, as aid for walking became necessary 10 to 15 years after disease onset (table 1).

The age at onset and disease course were apparently not correlated with the genotype. The c.430+3_430+6del variant shared by six individuals from four different families was identified in individual 1 who was wheelchair-bound before the age of 10, whereas

individual 4 was able to walk with aid at 26 years old. Like in most HSPs, other factors, genetic and/or environmental, may play a role in the phenotype. The recurrence of c.430+3_430+6del and the shared North African origin suggest a common haplotype, likely related to a founder effect. The two other variants identified in this study were found in only one family each.

As reported in the literature, no extra-neurological symptoms were noticed in this cohort. Thus, the alterations of ERLIN1 and the Erlin1/2-RNF170 module seem to be responsible for a purely neurological disorder, which is unexpected given their ubiquitous expression. In available expression databases (Ensembl, Gtex), three isoforms of ERLIN1 transcripts have been found in human tissues, ERLIN1-201, ERLIN1-202 and ERLIN1-203 (Figure S4), which differ by the size of their untranslated regions (Ensembl). ERLIN1-201 is poorly expressed in all tissues tested and the other isoforms are ubiquitously expressed, with low expression in the central nervous system (Gtex). Additionally, there is no enrichment or tissue-specific expression in the CNS. Thus, the expression pattern of ERLIN1 is not sufficient to explain the SPG62 phenotype.

What could explain brain involvement? The main role of the ERLIN1/2 complex is to recruit the E3 ubiquitin ligase RNF170 which subsequently degrades activated IP3R1, a receptor located at the ER membrane increasing cytosolic Ca2+ levels (Gao et Wojcikiewicz 2020; Prole et Taylor 2019). An alteration of this ERAD process would decrease IP3R1 degradation and further impair Ca2+ signaling, a mechanism known in neurodegeneration (Berridge 2016). IP3R1 is mainly expressed in the brain and the unique ablation of ERLIN1 expression is sufficient to increase IP3R1 levels by ~73% *in vitro* (Wright et al. 2018). Overall, despite a ubiquitous expression, these data are consistent with biallelic pathogenic variants in *ERLIN1* giving rise to a neurological disorder.

HSP is usually classified into two types depending on the phenotypic presentation, pure (an isolated pyramidal syndrome) and complex (pyramidal signs associated with additional neurological or systemic abnormalities) (Darios, Coarelli, et Durr 2022; Harding 1983). In the literature, only three SPG62 individuals from a single family carrying the homozygous p.(R255*) variant had complex forms of HSP, showing ataxia (3/3), dysarthria (1/3), and intellectual disability (2/3 with borderline intelligence)

(Novarino et al. 2014). Other individuals were reported with a pure form of HSP. Our series suggests that SPG62 could be associated with additional symptoms, i.e. superficial sensory loss and gait ataxia. The overall frequency of gait ataxia in SPG62 is almost 50% (43%, n=9/21). Although it is too early to state with certainty that SPG62 is associated with peripheral nerve involvement and/or cerebellar degeneration, an underlying mechanism implying both Erlin1/2-RNF170 module and IP3R1 degradation could be at play. The Erlin1/2-RNF170 module mainly degrades IP3R1, which is essentially expressed in the Purkinje cells of the cerebellum (Sharp et al. 1999; Gao et Wojcikiewicz 2020). Interestingly, pathogenic variants of *ITPR1,* the gene encoding for IP3R1, contribute to spinocerebellar ataxia 15 (SCA15, OMIM 606658), in which more than 85% of patients manifest gait ataxia and 40% pyramidal signs (Tipton et al. 2017). The description of more individuals as well as functional studies are needed to elucidate the SPG62 phenotypic spectrum.

In addition, ID does not appear to be a clear feature of SPG62, since only one person from our cohort had ID and two individuals from a single family have been previously reported as having borderline intelligence (Zhu et al. 2022). This is unexpected, because a majority of individuals who lost expression of the main ERLIN1 partner, i.e. persons with SPG18B due to biallelic *ERLIN2* pathogenic variants, were reported with ID (7/11 with available data) (Srivastava et al. 2020). Given the consanguinity in the studied families, we cannot rule out a hitherto unidentified recessive genetic variant, which would explain the cerebellar atrophy and ID in single individuals. Our study is the first to report brain anomalies in SPG62. About 40% of individuals from three distinct families had a TCC (5/13). Additionally, it is noteworthy that anomaly of the corpus callosum is a common feature of SPG18B (8/17). To determine whether SPG62 is associated with cerebellar atrophy and/or pontine hypersignal, as observed in one individual, additional patient descriptions are needed. Epilepsy was a feature in 3/17 persons with SPG18B (32), but only in one with SPG62. As previously discussed, a genotype-phenotype correlation is likely involved in the phenotypes associated with *ERLIN2*, with homozygous truncating variants inducing a more severe phenotype than missense variants (Srivastava et al. 2020), and monoallelic variants resulting in a pure, milder, and later-onset HSP (SPG18A) (Rydning et al. 2018; Park et al. 2020). Thus, there could be a dosage-dependent pathological mechanism for ERLIN2. Most likely, the common part of the phenotypes linked to pathogenic variants in the *ERLIN1* and

*ERLIN2* genes is related to the close interactions of their respective product in the ERLIN1/2 complex. The higher frequency of non-motor signs in SPG18B as compared to SPG62 suggests that the loss of ERLIN2 function has a more detrimental effect than that of ERLIN1 in the whole brain. This may be related to the ability of ERLIN2 to partially compensate for the loss of ERLIN1, whilst Erlin1 cannot compensate for the loss of ERLIN2, as previously shown *in vitro* (Wright et al. 2018; Hoegg et al. 2009). More studies are needed to fully characterize the phenotype of *ERLIN1* alterations and the overlapping mechanisms involved with the other partners of the Erlin1/2-RNF170 module.

## REFERENCES


Alazami, Anas M., Nouran Adly, Hisham Al Dhalaan, et Fowzan S. Alkuraya. 2011. « A Nullimorphic ERLIN2 Mutation Defines a Complicated Hereditary Spastic Paraplegia Locus (SPG18) ». *Neurogenetics* 12 (4): 333-36. https://doi.org/10.1007/s10048-011-0291-8.

Berridge, Michael J. 2016. « The Inositol Trisphosphate/Calcium Signaling Pathway in Health and Disease ». *Physiological Reviews* 96 (4): 1261-96. https://doi.org/10.1152/physrev.00006.2016.

Browman, Duncan T., Mary E. Resek, Laura D. Zajchowski, et Stephen M. Robbins. 2006. « Erlin-1 and Erlin-2 Are Novel Members of the Prohibitin Family of Proteins That Define Lipid-Raft-like Domains of the ER ». *Journal of Cell Science* 119 (Pt 15): 3149-60. https://doi.org/10.1242/jcs.03060.

Darios, Frédéric, Giulia Coarelli, et Alexandra Durr. 2022. « Genetics in Hereditary Spastic Paraplegias: Essential but Not Enough ». *Current Opinion in Neurobiology* 72 (février):8-14. https://doi.org/10.1016/j.conb.2021.07.005.

Daumke, Oliver, et Gary R. Lewin. 2022. « SPFH protein cage — one ring to rule them all ». *Cell Research* 32 (2): 117-18. https://doi.org/10.1038/s41422-021-00605-7.

Elsner, Leonie von, Guoliang Chai, Pauline E Schneeberger, Frederike L Harms, Christian Casar, Minyue Qi, Malik Alawi, et al. 2021. « Biallelic FRA10AC1 variants cause a neurodevelopmental disorder with growth retardation ». *Brain* 145 (4): 1551-63. https://doi.org/10.1093/brain/awab403.

Fagerberg, Linn, Björn M. Hallström, Per Oksvold, Caroline Kampf, Dijana Djureinovic, Jacob Odeberg, Masato Habuka, et al. 2014. « Analysis of the Human Tissue-Specific Expression by Genome-Wide Integration of Transcriptomics and Antibody-Based Proteomics ». *Molecular & Cellular Proteomics: MCP* 13 (2): 397-406. https://doi.org/10.1074/mcp.M113.035600.

Gao, Xiaokong, et Richard J. H. Wojcikiewicz. 2020. « The Emerging Link between IP3 Receptor Turnover and Hereditary Spastic Paraplegia ». *Cell Calcium* 86 (mars):102142. https://doi.org/10.1016/j.ceca.2019.102142.

Harding, A. E. 1983. « Classification of the Hereditary Ataxias and Paraplegias ». *Lancet (London, England)* 1 (8334): 1151-55. https://doi.org/10.1016/s0140-6736(83)92879-9.

Helms, J. Bernd, et Chiara Zurzolo. 2004. « Lipids as Targeting Signals: Lipid Rafts and Intracellular Trafficking ». *Traffic (Copenhagen, Denmark)* 5 (4): 247-54. https://doi.org/10.1111/j.1600-0854.2004.0181.x.

Hoegg, Maja B., Duncan T. Browman, Mary E. Resek, et Stephen M. Robbins. 2009. « Distinct Regions within the Erlins Are Required for Oligomerization and Association with High Molecular Weight Complexes ». *The Journal of Biological Chemistry* 284 (12): 7766-76. https://doi.org/10.1074/jbc.M809127200.

Iskender, Ceren, Ece Kartal, Fulya Akcimen, Cemile Kocoglu, Aslihan Ozoguz, Dilcan Kotan, Mefkure Eraksoy, Yesim G. Parman, et Ayse Nazli Basak. 2015. « Turkish Families with Juvenile Motor Neuron Disease Broaden the Phenotypic Spectrum of SPG11 ». *Neurology. Genetics* 1 (3): e25. https://doi.org/10.1212/NXG.0000000000000025.

Jm, de Sainte Agathe, Filser M, Isidor B, Besnard T, Gueguen P, Perrin A, Van Goethem C, et al. 2023. « SpliceAI-Visual: A Free Online Tool to Improve SpliceAI Splicing Variant Interpretation ». *Human Genomics* 17 (1). https://doi.org/10.1186/s40246-023-00451-1.

Kingsmore, Stephen F., Audrey Henderson, Mallory J. Owen, Michelle M. Clark, Christian Hansen, David Dimmock, Christina D. Chambers, Laura L. Jeliffe-Pawlowski, et

Charlotte Hobbs. 2020. « Measurement of Genetic Diseases as a Cause of Mortality in Infants Receiving Whole Genome Sequencing ». *NPJ Genomic Medicine* 5:49. https://doi.org/10.1038/s41525-020-00155-8.

Kircher, Martin, Daniela M. Witten, Preti Jain, Brian J. O'Roak, Gregory M. Cooper, et Jay Shendure. 2014. « A General Framework for Estimating the Relative Pathogenicity of Human Genetic Variants ». *Nature Genetics* 46 (3): 310-15. https://doi.org/10.1038/ng.2892.

Ma, Chengying, Chengkun Wang, Dingyi Luo, Lu Yan, Wenxian Yang, Ningning Li, et Ning Gao. 2022. « Structural Insights into the Membrane Microdomain Organization by SPFH Family Proteins ». *Cell Research* 32 (2): 176-89. https://doi.org/10.1038/s41422-021-00598-3.

Manganelli, Valeria, Agostina Longo, Vincenzo Mattei, Serena Recalchi, Gloria Riitano, Daniela Caissutti, Antonella Capozzi, Maurizio Sorice, Roberta Misasi, et Tina Garofalo. 2021. « Role of ERLINs in the Control of Cell Fate through Lipid Rafts ». *Cells* 10 (9): 2408. https://doi.org/10.3390/cells10092408.

Novarino, Gaia, Ali G. Fenstermaker, Maha S. Zaki, Matan Hofree, Jennifer L. Silhavy, Andrew D. Heiberg, Mostafa Abdellateef, et al. 2014. « Exome Sequencing Links Corticospinal Motor Neuron Disease to Common Neurodegenerative Disorders ». *Science (New York, N.Y.)* 343 (6170): 506-11. https://doi.org/10.1126/science.1247363.

Ouweneel, Amber B., Michael J. Thomas, et Mary G. Sorci-Thomas. 2020. « The Ins and Outs of Lipid Rafts: Functions in Intracellular Cholesterol Homeostasis, Microparticles, and Cell Membranes: Thematic Review Series: Biology of Lipid Rafts ». *Journal of Lipid Research* 61 (5): 676-86. https://doi.org/10.1194/jlr.TR119000383.

Park, Jin-Mo, Byeonghyeon Lee, Jong-Heun Kim, Seong-Yong Park, Jinhoon Yu, Un-Kyung Kim, et Jin-Sung Park. 2020. « An Autosomal Dominant ERLIN2 Mutation Leads to a Pure HSP Phenotype Distinct from the Autosomal Recessive ERLIN2 Mutations (SPG18) ». *Scientific Reports* 10 (1): 3295. https://doi.org/10.1038/s41598-020-60374-y.

Parodi, L., S. Fenu, G. Stevanin, et A. Durr. 2017. « Hereditary Spastic Paraplegia: More than an Upper Motor Neuron Disease ». *Revue Neurologique* 173 (5): 352-60. https://doi.org/10.1016/j.neurol.2017.03.034.

Pearce, Margaret M. P., Yuan Wang, Grant G. Kelley, et Richard J. H. Wojcikiewicz. 2007. « SPFH2 Mediates the Endoplasmic Reticulum-Associated Degradation of Inositol 1,4,5-Trisphosphate Receptors and Other Substrates in Mammalian Cells ». *The Journal of Biological Chemistry* 282 (28): 20104-15. https://doi.org/10.1074/jbc.M701862200.

Pearce, Margaret M. P., Duncan B. Wormer, Stephan Wilkens, et Richard J. H. Wojcikiewicz. 2009. « An Endoplasmic Reticulum (ER) Membrane Complex Composed of SPFH1 and SPFH2 Mediates the ER-Associated Degradation of Inositol 1,4,5-Trisphosphate Receptors ». *The Journal of Biological Chemistry* 284 (16): 10433-45. https://doi.org/10.1074/jbc.M809801200.

Pednekar, Deepa, Yuan Wang, Tatyana V. Fedotova, et Richard J. H. Wojcikiewicz. 2011. « Clustered Hydrophobic Amino Acids in Amphipathic Helices Mediate Erlin1/2 Complex Assembly ». *Biochemical and Biophysical Research Communications* 415 (1): 135-40. https://doi.org/10.1016/j.bbrc.2011.10.032.

« Predicting Splicing from Primary Sequence with Deep Learning - PubMed ». s. d. Consulté le 19 juin 2024. https://pubmed.ncbi.nlm.nih.gov/30661751/.

Prole, David L., et Colin W. Taylor. 2019. « Structure and Function of IP3 Receptors ». *Cold Spring Harbor Perspectives in Biology* 11 (4): a035063. https://doi.org/10.1101/cshperspect.a035063.

Rydning, S. L., A. Dudesek, F. Rimmele, C. Funke, S. Krüger, S. Biskup, M. D. Vigeland, et al. 2018. « A Novel Heterozygous Variant in ERLIN2 Causes Autosomal Dominant Pure Hereditary Spastic Paraplegia ». *European Journal of Neurology* 25 (7): 943-e71. https://doi.org/10.1111/ene.13625.

S, Chen, Francioli Lc, Goodrich Jk, Collins Rl, Kanai M, Wang Q, Alföldi J, et al. 2024. « A Genomic Mutational Constraint Map Using Variation in 76,156 Human Genomes ». *Nature* 625 (7993). https://doi.org/10.1038/s41586-023-06045-0.

Sharp, A. H., F. C. Nucifora, O. Blondel, C. A. Sheppard, C. Zhang, S. H. Snyder, J. T. Russell, D. K. Ryugo, et C. A. Ross. 1999. « Differential Cellular Expression of Isoforms of Inositol 1,4,5-Triphosphate Receptors in Neurons and Glia in Brain ». *The Journal of Comparative Neurology* 406 (2): 207-20.

Sobreira, Nara, François Schiettecatte, Corinne Boehm, David Valle, et Ada Hamosh. 2015. « New Tools for Mendelian Disease Gene Identification: PhenoDB Variant Analysis Module; and GeneMatcher, a Web-Based Tool for Linking Investigators with an Interest in the Same Gene ». *Human Mutation* 36 (4): 425-31. https://doi.org/10.1002/humu.22769.

Srivastava, Siddharth, Angelica D'Amore, Julie S. Cohen, Lindsay C. Swanson, Ivana Ricca, Antonella Pini, Ali Fatemi, Darius Ebrahimi-Fakhari, et Filippo M. Santorelli. 2020. « Expansion of the Genetic Landscape of ERLIN2-Related Disorders ». *Annals of Clinical and Translational Neurology* 7 (4): 573-78. https://doi.org/10.1002/acn3.51007.

Stevenson, Julian, Edmond Y. Huang, et James A. Olzmann. 2016. « Endoplasmic Reticulum-Associated Degradation and Lipid Homeostasis ». *Annual Review of Nutrition* 36 (juillet):511-42. https://doi.org/10.1146/annurev-nutr-071715-051030.

Thorvaldsdóttir, Helga, James T. Robinson, et Jill P. Mesirov. 2013. « Integrative Genomics Viewer (IGV): High-Performance Genomics Data Visualization and Exploration ». *Briefings in Bioinformatics* 14 (2): 178-92. https://doi.org/10.1093/bib/bbs017.

Tipton, Philip W., Kimberly Guthrie, Audrey Strongosky, Ronald Reimer, et Zbigniew K. Wszolek. 2017. « Spinocerebellar Ataxia 15: A Phenotypic Review and Expansion ». *Neurologia I Neurochirurgia Polska* 51 (1): 86-91. https://doi.org/10.1016/j.pjnns.2016.10.006.

Tunca, Ceren, Fulya Akçimen, Cemre Coşkun, Aslı Gündoğdu-Eken, Cemile Kocoglu, Betül Çevik, Can Ebru Bekircan-Kurt, Ersin Tan, et A. Nazlı Başak. 2018. « ERLIN1 Mutations Cause Teenage-Onset Slowly Progressive ALS in a Large Turkish Pedigree ». *European Journal of Human Genetics: EJHG* 26 (5): 745-48. https://doi.org/10.1038/s41431-018-0107-5.

Wagner, Matias, Daniel P. S. Osborn, Ina Gehweiler, Maike Nagel, Ulrike Ulmer, Somayeh Bakhtiari, Rim Amouri, et al. 2019. « Bi-Allelic Variants in RNF170 Are Associated with Hereditary Spastic Paraplegia ». *Nature Communications* 10 (1): 4790. https://doi.org/10.1038/s41467-019-12620-9.

Wiel, Laurens, Coos Baakman, Daan Gilissen, Joris A. Veltman, Gerrit Vriend, et Christian Gilissen. 2019. « MetaDome: Pathogenicity Analysis of Genetic Variants through Aggregation of Homologous Human Protein Domains ». *Human Mutation* 40 (8): 1030-38. https://doi.org/10.1002/humu.23798.

Wright, Forrest A., Caden G. Bonzerato, Danielle A. Sliter, et Richard J. H. Wojcikiewicz. 2018. « The Erlin2 T65I Mutation Inhibits Erlin1/2 Complex-Mediated Inositol 1,4,5-Trisphosphate Receptor Ubiquitination and Phosphatidylinositol 3-Phosphate

Binding ». *The Journal of Biological Chemistry* 293 (40): 15706-14. https://doi.org/10.1074/jbc.RA118.004547.
Young, Megan M., Mark Kester, et Hong-Gang Wang. 2013. « Sphingolipids: Regulators of Crosstalk between Apoptosis and Autophagy ». *Journal of Lipid Research* 54 (1): 5-19. https://doi.org/10.1194/jlr.R031278.
Zhu, Ze-Yu, Zi-Yi Li, Chao Zhang, Xiao-Li Liu, Wo-Tu Tian, et Li Cao. 2022. « A Novel Homozygous Mutation in ERLIN1 Gene Causing Spastic Paraplegia 62 and Literature Review ». *European Journal of Medical Genetics* 65 (11): 104608. https://doi.org/10.1016/j.ejmg.2022.104608.

## Statements and Declarations

**Funding:** The authors declare that no funds, grants, or other support were received during the preparation of this manuscript.

**Competing Interests:** The authors have no relevant financial or non-financial interests to disclose.

**Author Contributions:** Guillaume Cogan, Maha S. Zaki, Cyril Mignot contributed to the study conception and design. The clinical data of patients were provided by Maha S. Zaki, Mahmoud Issa, Florence Renaldo, Arnaud Isapof, Pauline Lallemant, Cécile Freihuber, Alexandra Durr and Cyril Mignot. The execution and the data analysis were performed by Guillaume Cogan, Boris Keren, Marine Guillaud-Bataille, Giovanni Stevanin, Lena Guillot-Noel, Thomas Courtin, Julien Buratti, Joseph G Gleeson, Robyn Howarth and Jean-Madeleine de Sainte Agathe. The first draft was written by Guillaume Cogan and Cyril Mignot, and all authors contributed to the edition of the final version.

**Data Availability:** The data generated during this study are available upon request to the corresponding author.

**Ethics approval:** This study was performed in line with the principles of the Declaration of Helsinki and was approved by authorization RBM-029 from the ethical institutional review board.

**Consent to participate:** Informed consent was obtained from all individual participants included in the study or the parents for individuals under 18.

**Consent to publish:** The authors affirm that human research participants provided informed consent for publication of their details.

**FIGURES and TABLES**

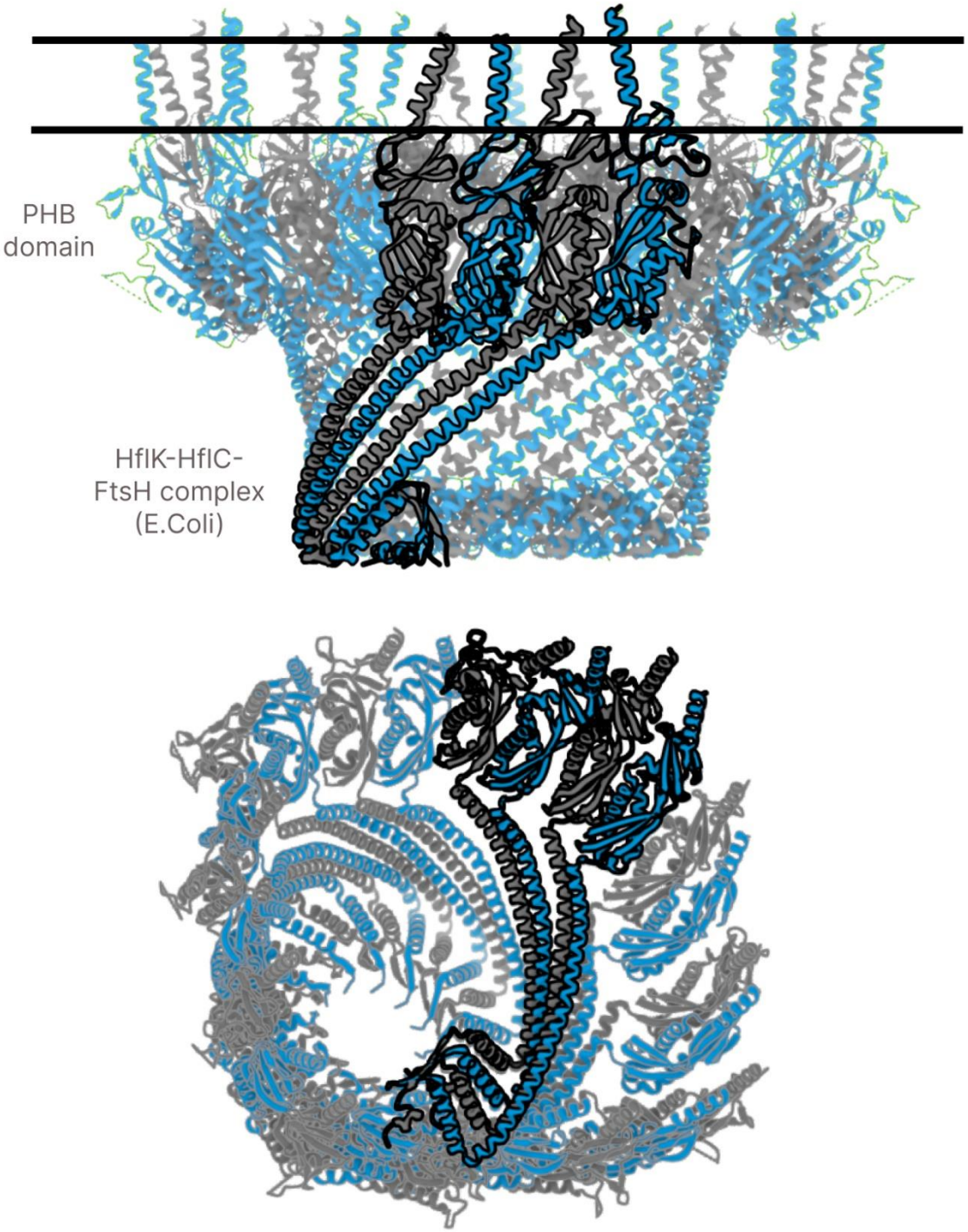


**Figure 1: 3D modeling of E.Coli FtsH complex**: structure of the FtsH complex in E coli (pdb: 7vhp), displaying the “bell-shaped” cage conformation of prohibitin homology (PHB) domain containing proteins, constituted by an assembly of lower-order Erlin1 (blue) and Erlin2 (grey) hetero-oligomers. The complex is anchored in a double layer membrane (black lines).

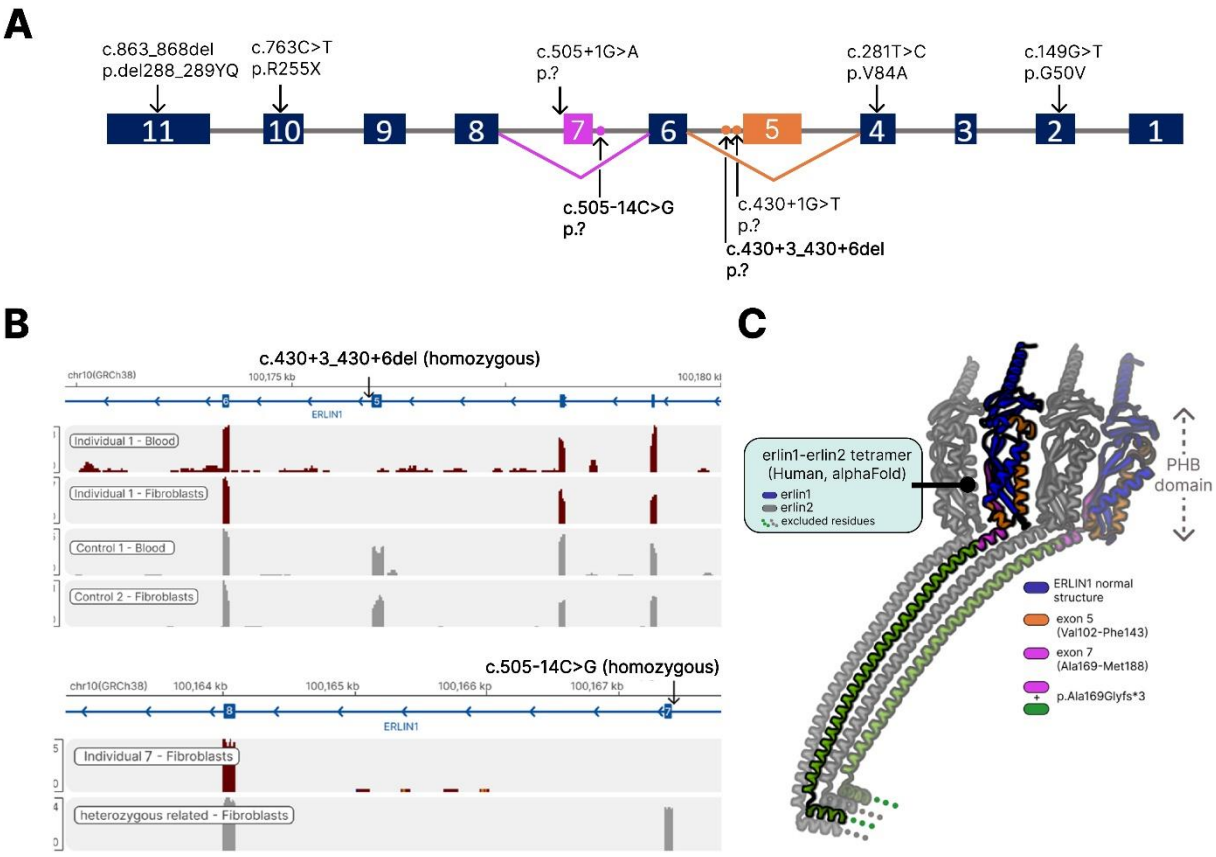


**Figure 2. *ERLIN1* mRNA structure, pathogenic variants and their consequences at the RNA and protein levels.** (A) Previously reported variants and variants reported in this article are noted above and below the protein, respectively. Intron 5 and intron 6 variants were predicted to generate a skipping of exon 5 (orange) and exon 7 (mangenta), respectively. (B) RNAseq analyses of RNA extracted from whole blood and fibroblasts of Individual 1 and from fibroblasts of Individual 7 confirmed a skipping of exon 5 (A, top two lines) and exon 7 (B, top line), respectively. (C): 3D structure of erlin1-erlin2 tetramer as predicted by AlphaFold. The C-terminal portion of erlin1/2 is not displayed for poor prediction quality reasons (plDDT < 50). The sequence encoded by exon 5 is in orange, exon 7 in magenta. The missing protein sequence predicted to result from p.Ala169Glyfs*3 is in magenta + green.


**Figure S1: Migration of the RT-PCR products of exon 5 (3' region) and exon 6 (5' region) of c.430+3_430+6del.** No amplification is visible in the two affected individuals whereas a 112 nucleotides product is seen in the control, meaning that the intronic c.430+3_430+6del skips exon 5.

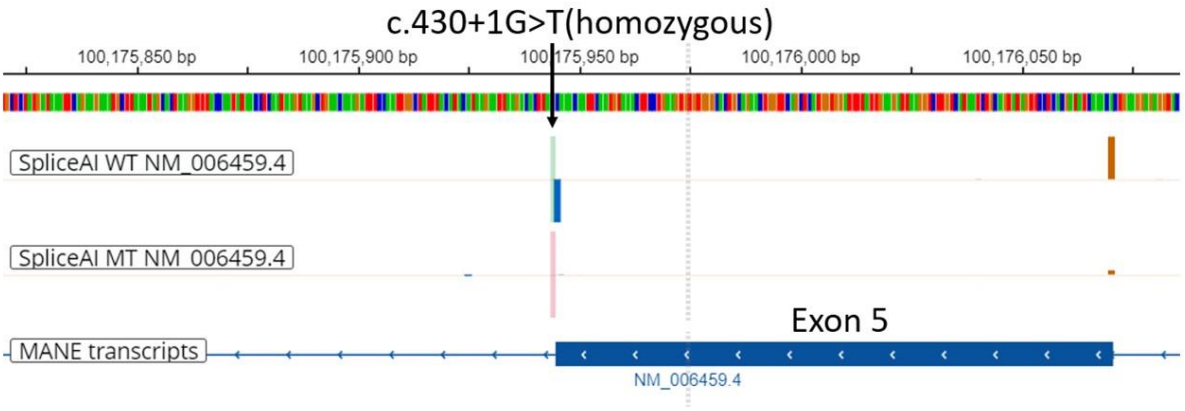


**Figure S2: SpliceAI-visual prediction of c.430+1G>T intronic variant.** SpliceAI visual predicts a donor loss of exon 5, leading to an exon 5 skipping (Donor Loss: 1, Donor gain 0.03, Acceptor gain and loss: 0).

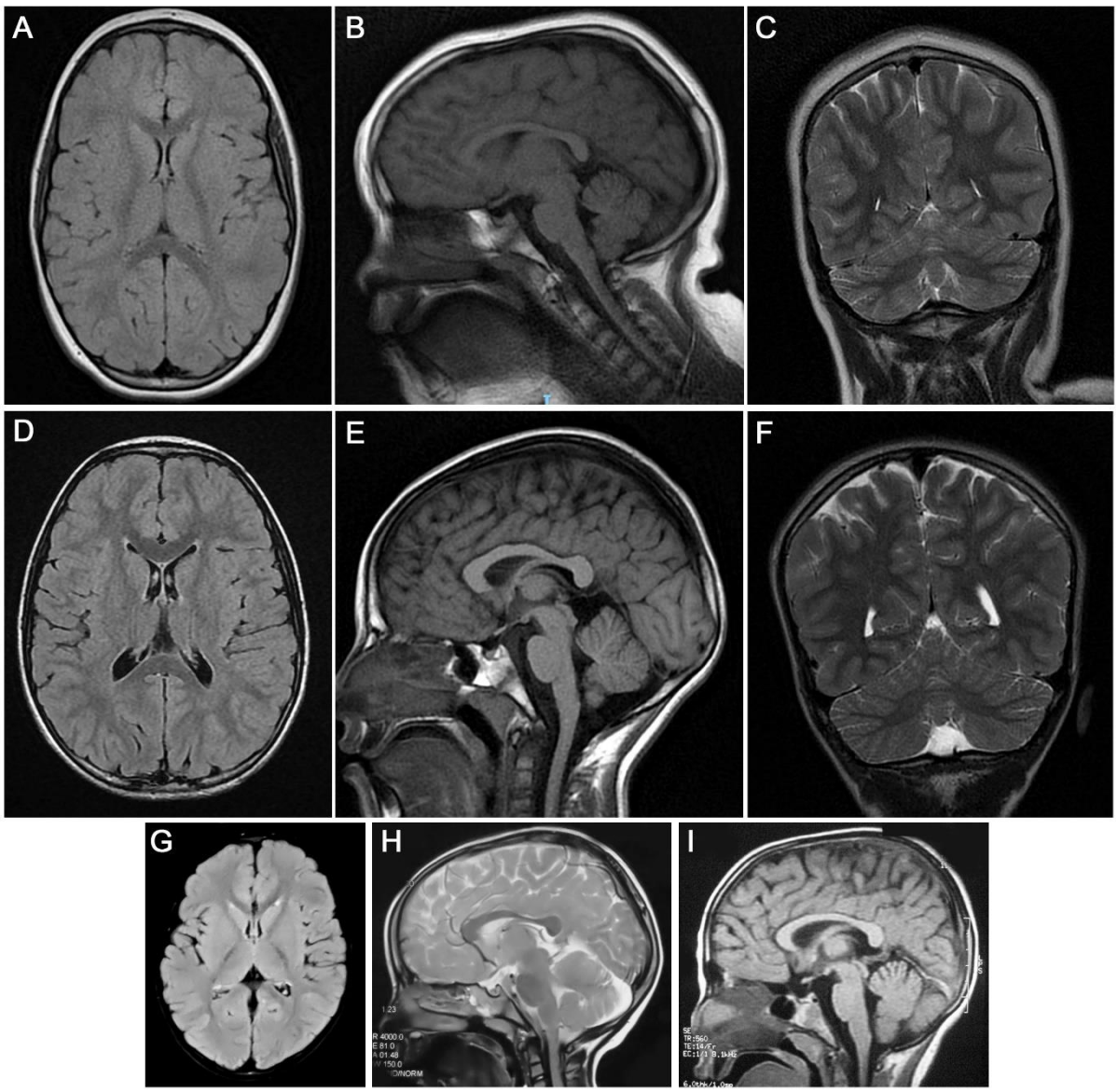


**Figure S3: Brain imaging of individuals with SPG62.** Brain MRI of individual I-1 (upper row), and IV-6 (lower row) showing FLAIR axial (A and D), midsagittal T1- (B and E) and coronal T2- (C and F) weighted images without anomalies. The lower row shows FLAIR axial (G) and midsagittal T2-weighted (H) MR images from individual III-5, as well as midsagittal T1-weighted (I) MR image from V-7, both having thin corpus callosum.

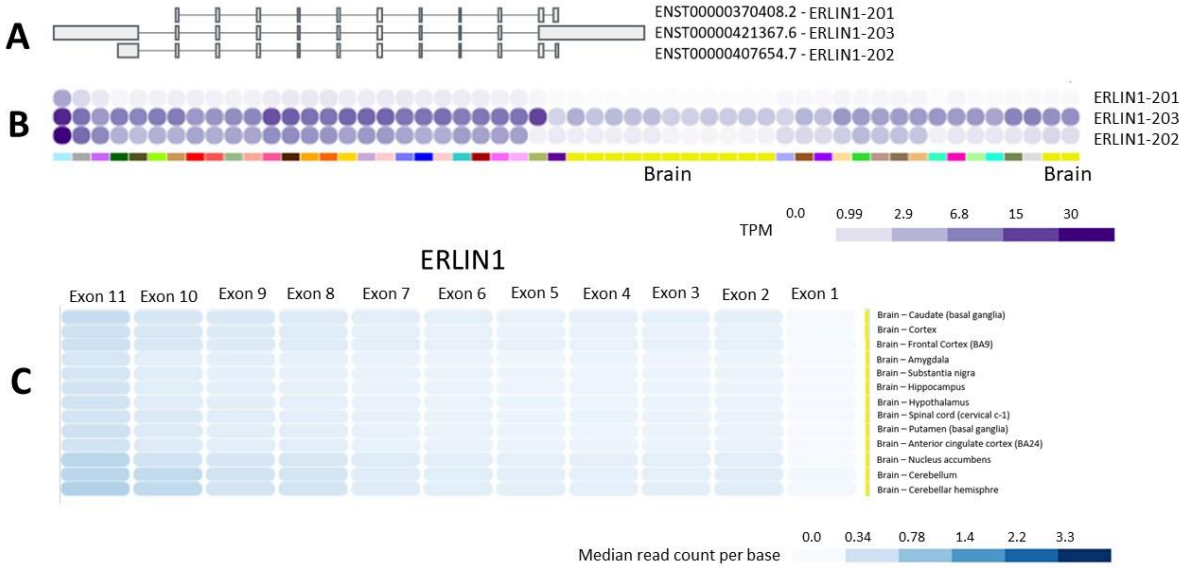


**Figure S4: Exploration of *ERLIN1* transcripts expression in the brain.**
(A) Three transcripts are described for *ERLIN1* (https://www.ensembl.org/Homo_sapiens/Gene/Summary?db=core;g=ENSG00000107566;r=10:100150094-100186033), they mainly differ by first and last exon size. (B) Each color represents a tissue / organ. ERLIN1-201 is poorly expressed while ERLIN1-202 and ERLIN1-203 are ubiquitously expressed, with a low level in brain structures (yellow) (https://www.gtexportal.org/home/transcriptPage). (C) No differential exon expression is manifest in brain structure.
TPM: Transcripts Per kilobase Million (TPM).

Table 1. Genetic and clinical data on 13 patients with biallelic *ERLIN1* variants and from previously reported cases

| **Family** | **I** | | **II** | | **III** | **IV** |
|---|---|---|---|---|---|---|
| **Individual** | 1 | 2 | 3 | 4 | 5 | 6 |
| **General data** | | | | | | |
| **Sex** | F | F | F | F | F | M |
| **Age at last examination (years)** | 9.8 | 22 | 18 | 26 | 6 | 11 |
| **Geographic origin** | North Africa | | North Africa | | North Africa / Middle East | North Africa |
| **Genetics** | | | | | | |
| **Consanguinity** | + | | + | | + | + |
| **Variant** | c.430+3_430+6delAAGT | | c.430+3_430+6delAAGT | | c.430+3_430+6delAAGT | c.430+3_430+6delAAGT |
| **Inheritance** | hmz | | hmz | | hmz | hmz |
| **Coding impact** | p.? | | p.? | | p.? | p.? |
| **Identification method** | ES | | ES | | ES | ES |
| **Further investigations** | RNA-seq | | PCR on RNA for II-3 and II-4 | | - | - |
| **Clinical data** | | | | | | |
| **Age at walking (months)** | 24 | 24 | 13 | 12 | 42 | 9 |
| **Age at first symptoms (months)** | 9 | 12 | 48 | 18 | NA | 24 |
| **First symptoms** | poor eye contact, global developmental delay | motor delay and stiff legs | NA | abnormal gait | delayed walking and abnormal gait | difficult tip toe walking |
| **LL pyramidal signs** | + | + | + | + | + | + |
| **UL pyramidal signs** | NA | NA | + | + | NA | - |
| **Gait ataxia** | - | + | - | - | - | - |
| **Motor deficit** | - | + | + | + | - | - |
| **Superficial sensory loss** | - | + | + | + | - | - |
| **Walking abilities (at last examination)** | wheelchair bound | walking difficulties without aid | uses 2 walking sticks | limited walking aid | NA | limited walking perimeter without aid (200 meters) |
| **Intellectual disability** | + | learning difficulties | NA | NA | learning difficulties | learning difficulties |
| **Language delay** | + | NA | NA | NA | - | - |
| **Behavioral disturbances** | + | NA | NA | NA | NA | - |
| **Seizures** | + | - | - | - | - | - |
| **Brain MRI findings** | - | cereb. atr. + pontine hypersignal | NA | TCC | TCC | - |
| **Oculomotor anomalies** | - | - | nystagmus | - | - | - |
| **Other** | | | | | | |
| **Urinary disturbances** | - | + | - | - | - | - |
| **Swallowing difficulties** | - | + | - | - | - | - |
| **Hyperlax joints** | - | - | + | - | - | - |
| **Scoliosis** | - | - | - | + | - | - |

Table 1 (continued)

| | | V | | | VI | | Literature* | Total |
|---|---|---|---|---|---|---|---|---|
| 7 | 8 | 9 | 10 | 11 | 12 | 13 | | |
| M | F | F | M | F | M | F | | |
| 7 | 38 | 37 | 29 | 40 | 5 | 2 | | |
| North Africa / Middle East | | | | | North Africa / Middle East | | | |
| + | | | | | + | | | |
| c.505-14C>G | | | | | c.430+1G>T | | | |
| hmz | | | | | hmz | | | |
| p.? | | | | | p.? | | | |
| GS | | | | | ES | | | |
| RNA-seq | | | | | - | | | |
| | | | | | | | | |
| NA | NA | NA | NA | 18 | 12 | 24 | NA | NA |
| NA | NA | NA | NA | NA | 12 | 24 | 58 (17 – 13y) | 41 (9-13y) |
| delayed walking and abnormal gait | delayed walking and abnormal gait | delayed walking and abnormal gait | delayed walking and abnormal gait | difficult tip toe walking | abnormal gait | tip toe walking | N/A | N/A |
| + | + | + | + | + | + | + | 8/8 | 21/21 |
| NA | NA | NA | NA | NA | NA | NA | NA | 2/3 |
| + | + | + | + | + | - | - | 3/8 | 9/21 |
| - | - | - | - | - | - | - | NA | 3/13 |
| - | - | - | - | - | - | - | 0/8 | 3/21 |
| NA | NA | NA | NA | NA | NA | NA | NA | N/A |
| - | NA | NA | NA | NA | - | - | 2/8 | 3/21 |
| - | NA | NA | NA | NA | + | - | NA | 2/6 |
| - | - | - | - | - | NA | NA | NA | 1/7 |
| - | - | - | - | - | - | - | 0/1 | 1/14 |
| TCC | TCC | TCC | NA | NA | NA | NA | 0/7 | 7/16 |
| - | - | - | - | - | - | - | NA | 1/13 |
| | | | | | | | | |
| - | - | - | - | - | - | - | 0/8 | 1/21 |
| - | - | - | - | - | - | - | 0/1 | 1/14 |
| - | - | - | - | - | - | - | NA | 1/13 |
| - | - | - | - | - | - | - | NA | 1/13 |

hmz: homozygous, ES: exome sequencing, WG: genome sequencing, NA: not available, N/A: not applicable, LL: lower limbs, UL: upper limbs, cereb. atr.: cerebellar vermis and hemisphere atrophy, TCC: thin corpus callosum. y: years

* We only considered individuals with a spastic paraplegia phenotype described in the literature (n=8).